MEAN FREE PATH DEPENDENCE OF THE TRAPPED FLUX SURFACE RESISTANCE*

M. Checchin†, M. Martinello, Fermilab, Batavia, IL 60510, USA and IIT, Chicago, IL 60616, USA
A. Grassellino, A. Romanenko, Fermilab, Batavia, IL 60510, USA
J.F. Zasadzinski, IIT, Chicago, IL 60616, USA

Abstract

In this article a calculation of the trapped flux surface resistance is presented. The two main mechanisms considered in such approach are the oscillation of the magnetic flux trapped in the superconductor due to the Lorentz force, and the static resistance associated to the normal conducting vortex core. The model derived shows a good description of the available experimental data, highlighting that the radio frequency vortex dissipation is mostly due to the static part of the surface resistance. We show that the surface resistance for 100% trapped flux normalized to the trapped field (expressed in nΩ/mG) can be approximated to $R_{flux}/B \approx 18.3(\mathrm{n}\Omega\sqrt{\mathrm{s\,nm}}/\mathrm{mG}) \cdot \left(\sqrt{l\,f}/\,(50.1(\mathrm{nm})+l)\right)$ with l the mean free path in nm and f the frequency in GHz.

INTRODUCTION

When the superconductive transition is performed in presence of external magnetic field, magnetic flux can be trapped in superconducting materials as energetically stable fluxoids in the mixed state of II type superconductors, or as vortexes pinned at defects in the Meissner state of I and II type superconductors. In some circumstances, magnetic flux lines can penetrate in the Meissner state without needing of pinning sites to exist in the so called intermediate state, as consequence of the demagnetization effect.

All such magnetic flux structures can introduce dissipation in both dc and radio frequency (RF) domains.

Controlling the pinning force of the superconducting material, it is possible to minimize the vortex dc dissipation, enabling superconductors to transport very high currents, without any dissipation, up to the depinning current.

On the other hand, in RF applications the vortexes dissipation is less controllable, and superconducting radio frequency (SRF) devices often operates in presence of such extra dissipation. The trapped flux problem is indeed critical for superconducting accelerating cavities, especially when high quality factors are needed for applications in continuous wave (CW) accelerators.

With the discovery of the nitrogen doping treatment [1] of SRF niobium cavities, it becames extremely important to deeply understand the origin of such extra dissipation. The nitrogen doping process modifies the niobium mean free path and energy gap [2, 3], introducing a beneficial effect on the quality factor Q_0, but at the same time it affects negatively the magnetic flux dissipation [4–6].

* Work supported by the US Department of Energy, Office of High Energy Physics.
† checchin@fnal.gov

In this work a model to describe the dissipation introduced by such flux structures in superconductors operating in RF field as a function of the mean free path is presented. The calculation will consider the following assumptions:

1. The vortex description is local
2. No interaction between vortexes are considered
3. $T << T_c$, no temperature dependencies are introduced
4. The single vortex resistance is defined as constituted by two contributions:
   (a) Static, due to the RF dissipation of the normal-conducting core
   (b) Dynamic, due to the Lorentz force acting on the flux
      - The pinning potential is approximated as parabolic
      - Only a single pinning point per vortex is considered
      - Every vortex experiences the same pinning potential
5. The applied magnetic field is 100% trapped during the superconductive transition.

In the non-local description, a vortex is described as a modulation of the order parameter of the superconductor tending to zero at the center of the vortex, and approaching to its finite value far from it [7].

Differently, in the local description introduced by C. Caroli *et al.* [8], the vortex is described as a normal conducting core with dimension of the order of the coherence length ξ_0. The superconducting currents that spin around it screening the magnetic flux confined inside.

In the model here presented, the dimension of the single vortex is described as in the work of J. Bardeen and M.J. Stephen [9]. The radius $a = \hbar/(2P_c)$ of the normal conducting core is defined as the distance from the center of the vortex at which the superelectrons' momentum assumes critical value P_c, and the superconducting energy gap Δ, otherwise constant at infinite, goes to zero.

In the clean limit where the electrons mean free path l is higher than the coherence length ξ_0 ($l > \xi_0$), the superelectrons' momentum critical value and the correspondent vortex radius are [9]

$$P_c = \frac{2.178\hbar}{2\pi\xi_0} \quad \rightarrow \quad a_{cln} = 1.16\xi_0 \qquad (1)$$

ISBN 978-3-95450-178-6

In the limit $l << \xi_0$ instead [9]

$$P_c = \sqrt{\frac{3\hbar^2}{4\pi l \xi_0}} \quad \rightarrow \quad a_{drt} = \sqrt{\frac{\pi}{3} l \xi_0} \tag{2}$$

From this description then, the dimension of the vortex's normal conducting core is strictly dependent on the electrons mean free path l, and accordingly to the two definition EQ. 1 and EQ. 2 will increase with $\sqrt{l}$ in the dirty limit, and will be constant in the clean limit.

DYNAMIC RESISTANCE

When magnetic flux is trapped at the RF surface, it experiences a force due to the interaction with the Eddy currents induced by the oscillating RF field [10–12]. The RF current density $\mathbf{j}(t) = \mathbf{j}cos(\omega t)$ exercises a force on the magnetic flux quantum ϕ_0 in the vortex, accordingly to the Lorentz force. The magnetic force acting on a single vortex per unit of length f_L is:

$$\begin{aligned} f_L &= |\mathbf{j} \times \phi_0 \hat{\mathbf{u}}_\mathbf{n}| \\ &= j\phi_0 sin(\theta) cos(\omega t) \end{aligned} \tag{3}$$

Where j is the RF current, θ the angle between $\mathbf{j}$ and $\phi_0 \hat{\mathbf{u}}_\mathbf{n}$ and ω the RF angular frequency.

We can write the motion equation of a single vortex subjected to the Lorentz force as follows:

$$M\ddot{x} = f_L + f_v + f_p + f_m \tag{4}$$

with M being the inertial mass of the vortex per unit of length as defined by J. Bardeen and M.J. Stephen [9]:

$$\begin{aligned} M &= 2\pi n m a^2 \left(\frac{H_{c2}}{H_f}\right) sin^2\alpha \quad ; \quad \phi_0 = \mu_0 H_f \pi a^2 \\ &= \frac{2\pi^2 \mu_0 n m a^4 H_{c2}}{\phi_0} sin^2\alpha \end{aligned} \tag{5}$$

where H_f is the magnetic flux in the vortex and α the Hall angle with respect the normal to $\mathbf{j}$ defined by

$$tan\alpha = \frac{e\phi_0\tau}{\pi m a^2}, \tag{6}$$

Table 1: Parameters values used in the simulations for niobium.

Parameter	Value	Reference
ξ_0	$39{\cdot}10^{-9}$ m	
λ_L	$23{\cdot}10^{-9}$ m	
H_{c2}	2400 Oe	[17]
v_f	$1.37{\cdot}10^{6}$ m/s	[16]
n	$5.56{\cdot}10^{28}$ m^{-3}	[16]
f	$1.3{\cdot}10^{9}$ Hz	

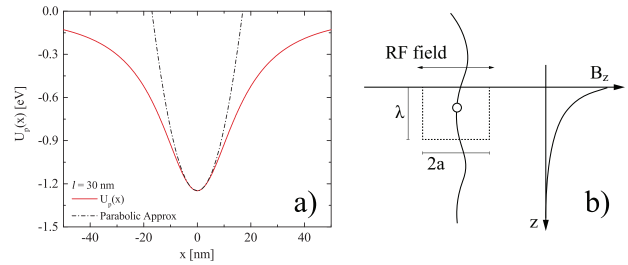

Figure 1: a) Lorentzian pinning potential and its parabolic approximation, b) sketch of the oscillating vortex pinned at the RF surface.

e and m are the charge and mass of the electron respectively, and $\tau = l/v_f$ the electron relaxation time, where v_f is the Fermi velocity.

The other forces acting on the vortex are f_p the pinning force, f_v the viscous drag force and f_m the Magnus force. The viscous drag force is defined as $f_L = -\eta\dot{x}$ where η is the vortex's motion viscosity per unit of length [13], defined as:

$$\eta = \frac{3}{2}\frac{\sigma_n \phi_0^2}{\pi^2 \xi_0 l} \tag{7}$$

where σ_n is the normal conducting resistivity ($\sigma_n = ne^2\tau/m$).

The description of the pinning force f_p is instead strictly related to the pinning potential U_p experienced by the vortex. The ideal pinning potential is function of the effective coherence length ξ and it is ideally described by an inverse Lorentzian function [14]. For vortex oscillations near the minimum of the potential the parabolic approximation can be used:

$$U_p = -\frac{U_0}{1 + (x/\xi)^2} \approx -U_0 + \frac{U_0 x^2}{\xi^2} \tag{8}$$

with U_0 the potential depth and $\xi = (1/\xi_0 + 1/l)^{-1}$. An example of such potential and its parabolic approximation are plotted in Fig. 1.

Knowing the pinning potential in EQ. 8, the pinning force normalized to the effective penetration depth λ is:

$$f_p = -\frac{2U_0 x}{\lambda\xi^2} = -px \quad ; \quad p = \frac{2U_0}{\lambda\xi^2} \tag{9}$$

where $\lambda = \lambda_L\sqrt{1 + (\xi_0/l)}$, and λ_L is the London penetration depth.

The Magnus force is defined as:

$$f_m = Cne|\mathbf{v} \times \phi_0 \hat{\mathbf{u}}_\mathbf{n}| \tag{10}$$

with n the electron density, and C the fraction of the Magnus force that is active. Usually the faction of active Magnus force is way littler than one, and can be neglected. Only for extremely pure superconductors this plays an important role [9, 12, 15]. The Magnus force will be therefore neglected in this calculation.

ISBN 978-3-95450-178-6

Substituting EQs. 3, 9, the viscous drag force with η equal to EQ. 7 in EQ. 4, and dividing by M, we get the motion equation of a single vortex:

$$\ddot{x} + \alpha \dot{x} + \beta^2 x = \gamma cos(\omega t) \tag{11}$$

which corresponds to a driven-dumped oscillator second order differential equation, with $\alpha = \eta/M$, $\beta^2 = p/M$ and $\gamma = j\phi_0 sin(\theta)/M$.

The solution of such differential equation is:

$$x(t) = x_0 cos(\omega t - \varphi) \tag{12}$$

where the phase lag φ and the amplitude x_0 are defined as:

$$\begin{aligned} tan\varphi &= \frac{\eta\omega}{p - M\omega^2} \\ x_0 &= \frac{j\phi_0 sin\theta}{\left[(p - M\omega^2)^2 + (\eta\omega)^2\right]^{1/2}} \end{aligned} \tag{13}$$

The instantaneous dissipated power by the oscillator driven by the Lorentz force f_L is defined as:

$$\begin{aligned} P(t) &= f_L(t) Re\{\dot{x}(t)\} \\ &= j\phi_0 sin\theta cos(\omega t) Re\{\dot{x}(t)\} \end{aligned} \tag{14}$$

So, the average dissipated power during one complete RF cycle is:

$$\langle P(t) \rangle = \frac{1}{T}\int_0^T P(t)dt \tag{15}$$

where T corresponds to the RF period equal to $2\pi/\omega$.

Solving the integral and substituting the oscillation amplitude x_0 defined in EQs. 13 we get:

$$\langle P(t) \rangle = \frac{1}{2}\frac{\omega\phi_0^2 sin^2\theta}{\left[(p - M\omega^2)^2 + (\eta\omega)^2\right]^{1/2}} j^2 \tag{16}$$

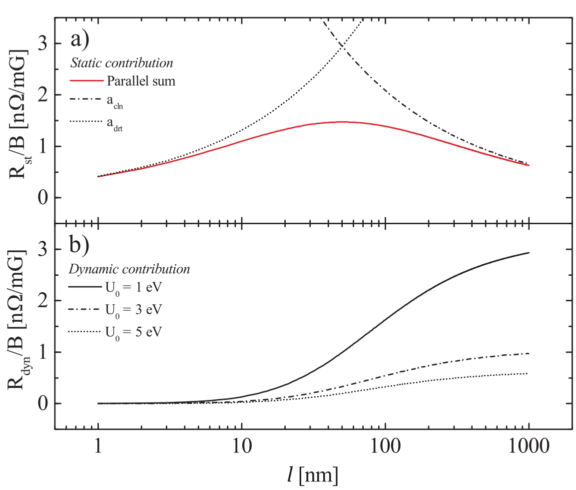

Figure 2: Resistance per mG of trapped magnetic field as a function of the mean free path: a) only static resistance, b) only dynamic resistance for different pinning potentials U_0.

The RF currents that flow at the superconducting surface will exponentially decay with constant λ inside the superconductor. We can therefore approximate that such currents will interact with the magnetic flux when passing through the surface of area $S_j = 2a\lambda$ (as sketched in Fig. 1b). We can write:

$$\begin{aligned} \langle P(t) \rangle &= \frac{1}{2}\frac{\omega\phi_0^2 sin^2\theta}{\left[(p - M\omega^2)^2 + (\eta\omega)^2\right]^{1/2}} \frac{I^2}{S_j^2} \quad ; \quad I = j \cdot S_j \\ &= \frac{1}{2} r_{dyn}^{single} \cdot I^2 \end{aligned}$$

so, the resistance per unit of length associated to a single vortex oscillating in the RF field is:

$$r_{dyn}^{single} = \frac{\omega\phi_0^2 sin^2\theta}{(2\lambda a)^2\left[(p - M\omega^2)^2 + (\eta\omega)^2\right]^{1/2}} \tag{17}$$

As defined in EQ. 1 and EQ. 2, a will correspond to the vortex radius in the clean limit or in the dirty limit depending on the mean free path l.

Considering now the specific case of SRF cavities, the RF currents **j** flow following the walls shape, encountering the magnetic flux contained in the vortexes with a random angle that spaces between $-\pi/2$ and $\pi/2$. We can then replace $sin^2\theta$ in EQ. 17 with its average 1/2.

Multiplying EQ. 17 by the effective penetration depth we can then define the dynamic resistance for single vortex as follows:

$$R_{dyn}^{single} = \frac{\omega\phi_0^2}{8\lambda a^2\left[(p - M\omega^2)^2 + (\eta\omega)^2\right]^{1/2}} \tag{18}$$

STATIC RESISTANCE

Since we are describing the vortex with the local model, besides the dissipation due to the oscillation of the vortex, we should consider also the dissipation due to its normal-conducting core. The dissipation will be then simply defined with the normal-conducting description of the surface resistance in presence of RF fields.

In the normal conductive case the oscillating electric field will be dumped inside the material within a length defined by the skin depth $\delta = \sqrt{2/(\mu_0\omega\sigma_n)}$. The normal-conducting resistance then will be:

$$R_{st}^{single} = \sqrt{\frac{\mu_0\omega}{2\sigma_n}} \tag{19}$$

In the case of the anomalous skin effect ($\delta < l$) this relation becomes:

$$R_{st}^{single} = \frac{4}{9}\left(\sqrt{3}\frac{\mu_0^2}{2\pi}\frac{l}{\sigma_n}\right)^{1/3}\omega^{2/3} \tag{20}$$

For niobium, the anomalous skin effect is reached when $l \gtrsim 500$ nm. Since for SRF cavities the usual mean free path ranges from about 1 nm to about 400 nm, in the present vortex resistance description we will limit our calculation to the normal skin effect only.

ISBN 978-3-95450-178-6

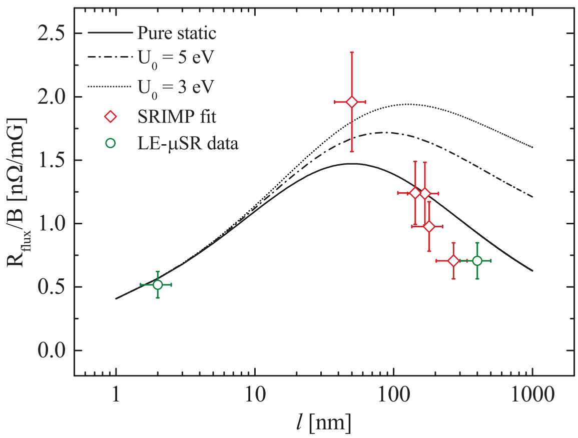

Figure 3: Experimental resistance per unit of trapped field data acquired for 1.3 GHz SRF cavities [4]. The three lines correspond to the simulations: solid line for pure static dissipation, dashed-dotted and dotted lines for total flux resistance calculated with two different pinning potentials.

TRAPPED FLUX SURFACE RESISTANCE

Till now we have derived the static and dynamic resistances associated to a single vortex. In case of a finite number of vortexes, we should multiply the resistance of a single vortex by a weight defined by the fraction of the total area occupied by vortexes.

For simplicity we should consider the case of 100% of magnetic flux trapped during the superconductive transition. In this scenario, if we apply a finite magnitude of magnetic field (H) to the superconductor during the transition, it will be subdivided in N vortexes, each one carrying magnetic flux ϕ_0 through an area πa^2 (with $a = a_{cln}, a_{drt}$).

Defining A as the normal conductive area that experiences the magnetic field right before the transition, the total magnetic flux that passes through that area will be:

$$A\mu_0 H = N\phi_0 \qquad (21)$$

and the fraction of the total area occupied by N vortexes $N\pi a^2/A$.

Multiplying this weight factor by the resistance of a single vortex, defined in EQs. 18 and 19, we obtain the resistance associated to N trapped vortexes in condition of pure static or pure dynamic dissipation:

$$R_{st,dyn} = \frac{\pi a^2 \mu_0}{\phi_0} H R^{single}_{st,dyn} \qquad (22)$$

In Fig. 2 the static and dynamic resistance components per mG of trapped field for many vortexes (EQ. 22) are plotted against the mean free path.

Table 1 reports all the parameters used in the simulations and respective references for niobium.

Figure 2a shows that the static resistance has an important dependence on the mean free path. In the dirty limit the vortex radius increases with the square root of l (EQ. 2), while the static single vortex resistance is proportional to $1/\sqrt{l}$ (EQ. 19). In the dirty limit then the static surface resistance will increase with the square root of the mean free path.

In the clean limit instead, the vortex radius does not depend on the mean free path (EQ. 1) and the static resistance will follow the the normal electron conductivity σ_n dependence on the mean free path, $\sigma_n \propto 1/\sqrt{l}$.

The best estimation of the static vortexes resistance has then to be considered equal to the parallel sum of the contribution in the clean and dirty limits (calculated using EQs. 1 and 2) represented by the solid line in Fig. 2a. The presence of these two limits, clean and dirty respectively, introduces two opposite dependencies on the mean free path implying the presence of a maximum in the convolution around 60 nm.

The dynamic part of the vortex resistance (Fig. 2b) has a different trend with the mean free path. The resistance values are lower than 0.1 nΩ/mG in the dirty limit ($l \lesssim 20$nm), so the dynamic contribution for low mean free path values is negligible. We can therefore approximate the vortex radius to EQ. 1 in the whole mean free paths range of interest.

For such contribution the main dependence on the mean free path is introduced by the pinning constant $p \propto 1/\left(\lambda\xi^2\right)$. In the dirty limit the coherence length is small ($\xi \simeq l$), while the penetration depth higher than the London penetration depth λ_L. The pinning constant is high for enough large U_0, so the vortex is well pinned and the dynamic dissipation negligible.

In the clean limit instead λ is very small, while the dominant term ξ increases tending to ξ_0. So, the pinning constant p becomes little as the material becomes cleaner, and as p decreases, the denominator of EQ. 18 decreases, implying an increment of the single vortex resistance. Such dependence is masked by the pinning potential depth though. If U_0 is big enough, and the frequency moderate, even for large mean free paths the dynamic resistance is negligible.

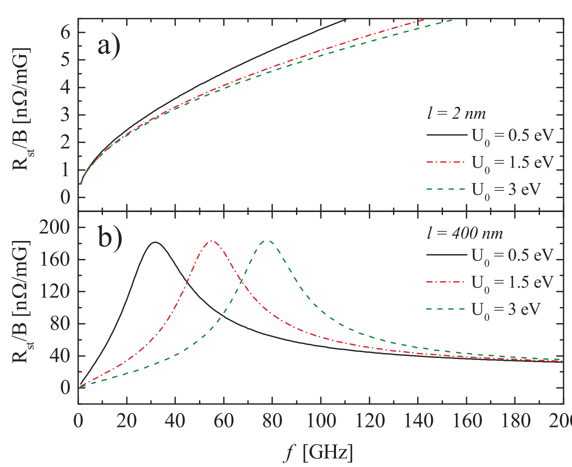

Figure 4: Resistance per mG of trapped field for different pinning potentials as a function of the frequency, for the dirty a) and clean b) limits respectively.

While the static resistance is always active even in dirty limit, the dynamic resistance is instead more appreciable in the clean limit when the pinning potential is swallow (U_0 small) as shown in Fig. 2b. The smaller U_0 the less bound is the vortex, and the bigger is the dynamic resistance associated to its motion.

The total flux surface resistance can be then defined as the superposition of the the resistance associated to the dynamic vortexes dissipation calculated in the clean limit, and the parallel sum of the static dissipation calculated in clean and dirty limits.

By using the definitions is EQs. 18, 19 and 22 we derive the 100% trapped flux surface resistance as a function of the applied magnetic field H during the transition, considering both dynamic and static resistances:

$$\begin{aligned} R_{flux} &= R_{dyn}^{cln} + \left(\frac{1}{R_{st}^{cln}} + \frac{1}{R_{st}^{drt}}\right)^{-1} \\ &= \frac{\pi\mu_0 H}{\phi_0}\left[\sqrt{\frac{\mu_0\omega}{2\sigma_n}}\left(\frac{a_{cln}^2 a_{drt}^2}{a_{cln}^2 + a_{drt}^2}\right) + \frac{\omega\phi_0^2}{8\lambda\left[(p - M\omega^2)^2 + (\eta\omega)^2\right]^{1/2}}\right] \end{aligned} \tag{23}$$

In Fig. 3 the surface resistance (EQ. 23) normalized to the magnetic field trapped in mG is plotted as a function of the mean free path for different values of pinning potential.

The data points plotted with the simulation of Fig. 3 are experimental points measured at 16 MV/m for niobium 1.3 GHz SRF cavities as explained in M. Martinello *et al.* work [4]. Green void circles correspond to mean free path values obtained via low energy muon spin rotation (LE-μSR) measurements [18], while red void diamonds to mean free path values obtained by measurement of the cavity frequency variation as function of the temperature with a SRIMP-based method [4, 19, 20].

The figure shows that the simulation describes consistently the experimental data trend. In particular the model highlights that the dynamic component of the surface resistance is not the principal factor in the description of the trapped flux surface resistance. The simulation in Fig. 3 that better describe the experimental data trend corresponds to pure static dissipation (solid line).

This means that the principal cause that introduces vortexes dissipation in RF superconducting applications is the static contribution to the surface resistance. The dynamic part is still present but negligible in the case of enough strong pinning.

The trapped flux resistance as a function of the RF frequency for dirty and clean limits is plotted in Fig. 4.

In the dirty limit the resistance is governed by the static contribution, and the total trapped flux resistance scales as $\sqrt{\omega}$ as shown in Fig. 4a. As expected, some deviations from the square root frequency dependence are observable in case of weak pinning as the frequency increases.

In the clean limit instead, the dynamic resistance plays an important role, and the resistance has a more complicated frequency dependence (Fig. 4b). In particular when the RF frequency is equal to the intrinsic vortexes oscillation frequency $\omega_0 = \sqrt{p/M}$ the resonance condition is matched and the flux resistance increases drastically. The resonance peak is well observable in Fig. 4b. The stronger the pinning, the higher the resonance frequency and the narrower the resonance peak.

Such resonant condition is not usually observed at the frequencies normally implemented in SRF applications, inasmuch achievable only at very high frequencies, or in case of very weak pinning.

CONCLUSIONS

In this work we have derived the RF surface resistance introduced by magnetic vortexes trapped in superconducting niobium in the Meissner state.

We have shown that the trapped flux surface resistance, in presence of pinning, is well approximated by the static resistance introduced by the vortexes normal conducting cores as a function of the mean free path.

Neglecting the dynamic resistance, the 100% trapped flux surface resistance (EQ. 23) normalized to the trapped magnetic field in nΩ/mG can be approximated to:

$$\frac{R_{flux}}{B} \approx 18.3\left(\frac{\text{n}\Omega\sqrt{\text{s}}\,\text{nm}}{\text{mG}}\right)\cdot\frac{\sqrt{l\,f}}{50.1(\text{nm}) + l}$$

where f is the frequency in GHz and l the electrons mean free path in nm.

It was found that the frequency proportionality depends on the mean free path and on the grade of pinning. In case of strong pinning we found a square root dependence of the trapped flux resistance in the dirty limit, while in the clean limit a resonant behavior of the trapped flux resistance is predicted for high frequencies.

Concluding, such description of the magnetic flux trapped surface resistance can be considered a good approximation, since able to predict the trend experimentally found.

ISBN 978-3-95450-178-6

REFERENCES

[1] A. Grassellino *et al.*, Supercond. Sci. Technol. **26** 102001 (2013).

[2] A. Grassellino *et al.*, **MOBA06**, Proceedings of 17th International Conference on RF Superconductivity, Whistler, Canada (2015).

[3] A. Grassellino *et al.*, **MOPB029**, Proceedings of 17th International Conference on RF Superconductivity, Whistler, Canada (2015).

[4] M. Martinello *et al.*, **MOPB015**, Proceedings of 17th International Conference on RF Superconductivity, Whistler, Canada (2015).

[5] S. Posen *et al.*, **MOPB104**, Proceedings of 17th International Conference on RF Superconductivity, Whistler, Canada (2015).

[6] D. Gonnella, M. Liepe, Proceedings of 27th Linear Accelerator Conference, Geneva, Switzerland (2014)

[7] A.A. Abrikosov *Fundamentals of the Theory of Metals*, North-Holland (1988).

[8] C. Caroli, P.G. de Gennes, J. Matricon, Phys. Lett. **9**, 307 (1964).

[9] J. Bardeen, and M.J. Stephen, Phys. Rev. **140**, A1197 (1965).

[10] A. Gurevich, G. Ciovati, Phys. Rev. B **87**, 054502 (2013).

[11] M. Rabinowitz, J. App. Phys. **41**, 88 (1971).

[12] R.P. Huebener *Magnetic Flux Structures in Superconductors*, Second Ed., Sringer-Verlag Berlin Heidelberg GmbH (2001).

[13] Y.B. Kim, C.F. Hempstead, and A.R. Strnad, Phys. Rev. **139**, A1136 (1965).

[14] L. Embon *et al.*, Sci. Rep. (2015) DOI: 10.1.38/srep07598.

[15] R.P. Huebener, A. Seher, Phys. Rev. **181**, 701 (1969).

[16] N.W. Ashcroft, N.D. Mermin *Solid State Physics*, Harcourt College Publishers (1976).

[17] H. Padamsee, J. Knobloch, T. Hays *RF Superconductivity for Accelerators*, Whiley-VCH Verlag GmbH & Co. KGaA (2008).

[18] A. Romanenko, A. Grassellino, F. Barkov, A. Suter, Z. Salman, T. Prokscha, Appl. Phys. Lett. **104**, 072601 (2014).

[19] J. Halbritter, Z. Physik **236**, 466 (1970).

[20] S. Meyers, S. Posen, M. Liepe, Proceedings of 27th Linear Accelerator Conference, Geneva, Switzerland (2014).